Optik xxx (2010) xxx–xxx

Contents lists available at ScienceDirect

Optik

journal homepage: www.elsevier.de/ijleo

The homogeneous problem for a corrugated metamaterial of arbitrary permittivity and permeability: Choosing the proper Riemann surface

Mauro Cuevas*, Ricardo A. Depine

Grupo de Electromagnetismo Aplicado, Departamento de Física, Facultad de Ciencias Exactas y Naturales, Universidad de Buenos Aires, Ciudad Universitaria Pabellón I, 1428, Buenos Aires, Argentina

ARTICLE INFO

Article history:
Received 17 June 2009
Accepted 5 December 2009
Available online xxx

Keywords:
Surface polaritons
Plasmonics
Diffraction
Grating
Negative refraction

ABSTRACT

To obtain the eigenmodes of the electromagnetic field at a periodically corrugated metamaterial we consider the analytic extension to the complex plane of the solution to the boundary-value problem for a metamaterial grating. We build a proper Riemann sheet for these eigenmodes and we present numerical examples illustrating their propagation characteristics. Particularly, we pay special attention to regimes corresponding to ideally transparent metamaterials with a negative index of refraction, where the eigenmodes can radiate into the metamaterial medium.

1. Introduction

A surface electromagnetic wave is a confined mode of propagation along an interface separating two media. These modes are obtained as a solution to the so-called homogeneous problem, in other words, they are a solution to Maxwell's equations and appropriate boundary conditions with no incident wave. The simplest case of a surface mode is that of a plane interface separating two isotropic media with constitutive parameters ε_1, μ_1 (medium 1) and ε_2, μ_2 (medium 2). In the ideal lossless case (ε_1, μ_1, ε_2 and μ_2 real) these surface modes are known as Fano's modes [1,2]. Interest in this subject has long been motivated by surface plasmons [3], surface modes with *p* polarization that appear when the media have dielectric permittivities ε_1 and ε_2 with opposite signs, since only these surface modes can exist in conventional isotropic media (positive magnetic permeabilities). In addition to surface modes with *p* polarization, a plane surface can also support surface modes with *s* polarization when the media have magnetic permeabilities with opposite signs [4]. The recent advent of artificial media [5–8] with negative refractive index (constitutive parameters simultaneously negative in the same frequency range) has aroused new interest in the study of the homogeneous problem of a surface. Solutions with novel characteristics, such as negative phase velocity opposed to group velocity, have been reported in Refs. [4,9,10].

The effect of media losses on the propagation characteristics of the eigenmodes in a plane interface has been studied by Ishimaru et al. [11]. In this case, the surface modes are also known as Zenneck's propagation modes. Since the constitutive parameters of media with losses are complex numbers, the propagation constant of a surface wave is also complex and the surface mode loses energy as it propagates. While it could be argued that losses in an absorbent medium could be an obstacle for surface mode propagation, this is not always so. For example, Yang et al. [12] have found long-range modes (that is, modes with a propagation constant having a small imaginary part) in a slab of a non-magnetic material, with a real part of the electric permittivity much smaller than its imaginary part. In these modes, which appear when the slab thickness is much smaller than the wavelength of the surface mode, the imaginary part of the propagation constant is inversely proportional to the imaginary part of the dielectric permittivity of the material.

Unlike Fano's modes, which exist even in the ideal case of non-absorbent media [2], media losses are essential for the existence of other surface modes. This is the case of Brewster–Zenneck's (BZ) modes [13] and CSW modes (acronym for complex surface wave) [14,15]. If one of the media is vacuum (ε_1=μ_1=1), BZ modes appear when $0 \leq \mathrm{Re}\,\varepsilon_2 < 1$ and $\mathrm{Im}\,\varepsilon_2 > \mathrm{Re}\,\varepsilon_2\,[(1+\mathrm{Re}\,\varepsilon_2)/(1-\mathrm{Re}\,\varepsilon_2)]^{1/2}$, while CSW modes appear when $\mathrm{Re}\,\varepsilon_2 > 0$ and $\mathrm{Im}\,\varepsilon_2 > 1$. Both modes play a key role in the extraordinary transmission phenomenon [13–15].

When focusing on the key aspects of the propagation, ideal lossless materials are usually assumed, although the dispersive nature of the media necessarily implies the existence of dissipation. In

* Corresponding author.
E-mail addresses: cuevas@df.uba.ar (M. Cuevas), rdep@df.uba.ar (R.A. Depine).

0030-4026/$ – see front matter © 2010 Elsevier GmbH. All rights reserved.
doi:10.1016/j.ijleo.2009.12.010

these cases, the propagation constant for a flat surface is real. Furthermore, since the field amplitudes decrease exponentially with the distance to the surface, the propagation constant must be larger than the absolute value of the photon's wave vector in both media. This condition prevents the excitation of a surface mode with a plane wave in a plane surface, as the phase velocity of the surface mode is always lower than the speed of light in the media separated by the surface. Therefore, in order to excite and detect surface modes, we must resort to special phase-coupling techniques, in which the simple configuration of a single plane interface must necessarily be abandoned. The most popular coupling techniques [2,3] are based on the use of attenuated total reflection or the use of a diffraction grating. It should be noted that in these cases, the coupling can be observed because the change of geometry modifies the propagation constant. This means that, in the case of lossless media, its imaginary part is no longer null. Once the surface mode has been excited, this imaginary part produces radiation losses, and the radiated energy can significantly modify the response of the surface as compared with the non-excitation case, thus allowing the detection of the surface mode.

In a recent work [16] we have used the grating coupling technique to study the resonant detection of the surface modes of a metamaterial illuminated by a plane wave. Although the findings obtained in this work give an idea of how corrugation modifies the propagation of surface waves, the homogeneous problem must be solved in order to carry out a thorough study. This homogeneous problem is, in many aspects, formally similar to the one considered in [16], although it does present additional difficulty related to the analytic continuation of certain physical quantities in the complex plane. Analytic continuation is inevitable, even in the case of media with no intrinsic losses, since corrugation modifies the propagation constant of the surface wave and may generate non-null imaginary parts. Specifically, it is essential to determine the branches of Riemann surface for the function that gives the propagation constant perpendicular to the surface in terms of the propagation constant parallel to the surface.

Although the cuts which determine the different branches of a multivalued function are arbitrary in principle, the choice of the most adequate cut depends on the specific physical problem. More than one cut has been suggested in the literature for the study of proper modes. In references [11,17–19], the cut lines are chosen so that the imaginary parts of the propagation constants perpendicular to the surface are zero, while the branches of the square root function are chosen so that the field of the proper mode is bound to the surface. This is the cut chosen by Ishimaru et al. [11] to extend the homogeneous problem of the plane interface of a metamaterial with arbitrary refractive index considered in [4,9,10] to media with losses. However, with the cuts described in Ref. [20], the proper modes are those whose propagation constants parallel to the surface have a larger real part than the photon's wave vector in each of the media (non-radiative modes).

The aim of this paper is to clarify the most adequate selection criteria to study how the propagation characteristics of surface modes change when the plane surface between a conventional dielectric material and a metamaterial with negative refractive index is periodically perturbed. Particularly, we will only consider proper modes whose existence does not require intrinsic losses (Fano's modes). In Section 2 we discuss the cuts proposed in [11] and show that these cuts are not adequate to determine the proper modes of the problem of a periodically corrugated surface, since they do not provide the expected radiation field for certain values of the wavelength to period ratio. We also show that the adequate cuts to describe the problem must be similar to those proposed in references [20,23]. In Section 3, we obtain the proper modes for the case of a metamaterial with negative refractive index. We demonstrate that the surface mode loses energy only through radiation and that this energy can be radiated towards either the dielectric material or the medium. As a result, a power flux normal to the mean plane of the surface appears. Depending on the propagation characteristics of the surface wave, this can be an incoming or an outgoing flux.

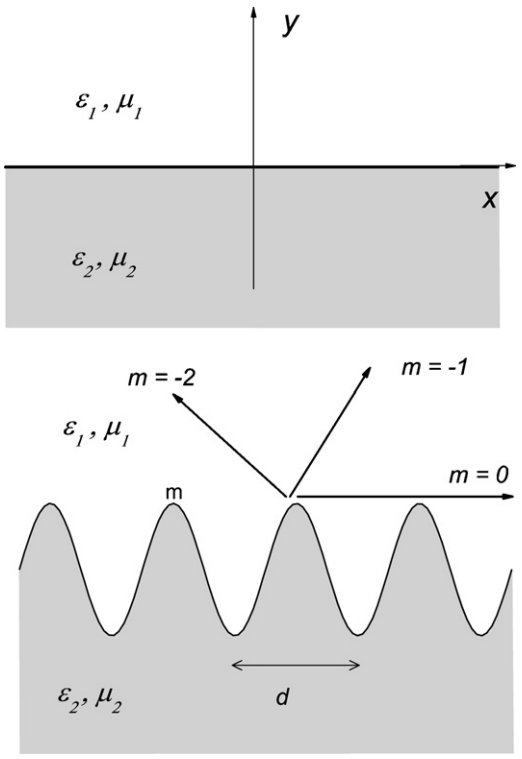

Fig. 1. (a) Plane surface $y = 0$ separating an ideal dielectric material with constitutive parameters ε_1, μ_1 from another material with constitutive parameters ε_2, μ_2. (b) Periodically corrugated boundary represented by $y = f(x)$. The spatial harmonic $m = 0$ is nonradiative, while harmonics $m = -1$ and $m = -2$ radiate into medium 1.

2. Determining the Riemann physical surface

Let us consider the plane surface $y = 0$ (Fig. 1a) which separates an ideal dielectric material with constitutive parameters ε_1, μ_1, both real and positive, from another material with constitutive parameters ε_2, μ_2 with real parts arbitrarily assigned and imaginary parts much smaller than the absolute value of the real part. If $\phi(x, y)$ represents the z component of the total magnetic field for the p polarized mode or the total electric field for the s polarized mode, the field on either side of this surface is written as

$$\phi(x, y) = R\, e^{i(\alpha x + \beta^{(1)} y)}, \quad y > 0 \tag{1}$$

$$\phi(x, y) = T\, e^{i(\alpha x - \beta^{(2)} y)}, \quad y < 0, \tag{2}$$

where R and T are complex amplitudes, α is the propagation constant parallel to the surface and $\beta^{(1)}$ and $\beta^{(2)}$ are the transverse components of the wave vector in each media. In terms of the dimensionless propagation parameter κ, $\alpha = 2\pi/\lambda\kappa$, where λ is the wavelength in medium 1 and

$$\beta^{(1)} = \frac{2\pi}{\lambda}(1 - \kappa^2)^{1/2}, \tag{3}$$

$$\beta^{(2)} = \frac{2\pi}{\lambda}(n^2 - \kappa^2)^{1/2}, \tag{4}$$

with $n = \sqrt{\varepsilon_2}\sqrt{\mu_2}/\sqrt{\varepsilon_1\mu_1}$ being the relative refractive index. The bivalued nature of functions $\beta^{(j)}$ $(j = 1, 2)$ requires determining those branches which have physical sense. To ensure the radiation conditions in the infinity when κ is real, these branches are chosen

Please cite this article in press as: M. Cuevas, R.A. Depine, The homogeneous problem for a corrugated metamaterial of arbitrary permittivity and permeability: Choosing the proper Riemann surface, Optik - Int. J. Light Electron Opt. (2010), doi:10.1016/j.ijleo.2009.12.010

by imposing conditions

$$\mathrm{Im}\,\beta^{(j)} \geq 0, \tag{5}$$

so that, in their respective complex planes, functions $\beta^{(j)}(\kappa)$ always move along the curves $\delta^{(j)}$ represented by dotted lines in Fig. 2b and d. When κ is a complex number, curve $\delta^{(j)}$ must fall in the region of the complex plane corresponding to the physical branch of function $\beta^{(j)}(\kappa)$ and, therefore, this branch must satisfy condition (5) for complex κ.

Branches $\mathrm{Im}\,\beta^{(1)} \geq 0$ and $\mathrm{Im}\,\beta^{(2)} \geq 0$ define the *proper sheet* (also known as physical sheet) on the Riemann surface in the complex space κ. The Riemann surface also includes three other sheets (called improper sheets because they do not represent physically acceptable waves) corresponding to the following choice of branches: $\mathrm{Im}\,\beta^{(j)} < 0$ for $j = 1, 2$, $\mathrm{Im}\,\beta^{(1)} < 0$ y $\mathrm{Im}\,\beta^{(2)} > 0$, $\mathrm{Im}\,\beta^{(1)} > 0$ and $\mathrm{Im}\,\beta^{(2)} < 0$. The four sheets (one proper and three improper sheets) are separated from each other by condition $\mathrm{Im}\,\beta^{(j)} = 0$, which can be explicitly rewritten as:

$$\kappa^2 - n^{(j)2} = -a, \tag{6}$$

with real and positive a and where $n^{(1)} = 1$ and $n^{(2)} = n$. Eq. (6) defines the cut lines in the complex space κ shown with symbol L_j in Fig. 2a and c. Each line divides the complex plane κ into two regions. As shown in Fig. 2a, line L_1 divides regions Γ_1 (dark grey) and Γ_{II} (light grey). Analogously, line L_2 (see Fig. 2c) divides regions Ω_I (dark grey) and Ω_{II} (light grey).

We now proceed to perturb the plane surface with a small periodical corrugation represented by function $y = f(x)$ (see Fig. 1b). In this case, the field $\phi(x, y)$ can be developed as a series of spatial harmonics (or orders)

$$\phi(x,y) = \sum_{m=-\infty}^{+\infty} R_m\, e^{i(\alpha_m x + \beta_m^{(1)} y)}, \quad y > \max\{f(x)\}, \tag{7}$$

$$\phi(x,y) = \sum_{m=-\infty}^{+\infty} T_m\, e^{i(\alpha_m x - \beta_m^{(2)} y)}, \; y < \min \quad \{f(x)\}, \tag{8}$$

where

$$\alpha_m = \frac{2\pi}{\lambda}\kappa\left(\frac{h}{\lambda}\right) + \frac{2\pi}{d}m, \tag{9}$$

is the x component of the wave vector of the m th spatial harmonic, h is the corrugation height, $\kappa(h/\lambda)$ is the dimensionless propagation constant corresponding to $m = 0$ and d is the corrugation period. The y component of the wave vector of the m th spatial harmonic is

$$\beta_m^{(1)} = \frac{2\pi}{\lambda}(1 - \kappa_m^2)^{1/2} \tag{10}$$

$$\beta_m^{(2)} = \frac{2\pi}{\lambda}(n^2 - \kappa_m^2)^{1/2}. \tag{11}$$

As the surface wave propagates along the surface, the spatial harmonics can radiate energy towards medium 1 as long as condition $|\mathrm{Re}\,\kappa_m| < 1$ is verified. The number of radiative spatial harmonics depends on the λ/d relation.

In Fig. 1b, we have outlined a situation with two propagating orders. Our aim is to see whether the cut defined for the case of a plane surface correctly describes this situation. Unlike the case of a flat surface, we now have an infinite set of *Riemann physical sheets*, one for each spatial harmonic corresponding to Eq. (8). This set constitutes the Riemann's physical sheet of the homogeneous problem of a corrugated surface. If the cut given by Eq. (6) is generalized to the complex plane κ_m of each spatial harmonic, and if branches of functions $\beta_m^{(j)}$ are chosen in a similar way to that used for the case of a plane surface, they satisfy the following condition

$$\mathrm{Im}\,\beta_m^{(j)} \geq 0. \tag{12}$$

With this generalization, both the cut lines in the complex plane corresponding to the spatial harmonic κ_m as well as the branches of functions $\beta_m^{(j)}$ are identical to those shown in Fig. 2, except that κ must now be replaced with κ_m and $\beta^{(j)}$ must be replaced with $\beta_m^{(j)}$. The infinite set of planes κ_m whose image through functions $\beta_m^{(j)}$ is determined by conditions (12) constitutes the Riemann physical sheet of the problem. We shall see that this choice does not show the expected radiation mechanism for the surface wave, even in the case of a metallic surface. In this case, it is well known that the

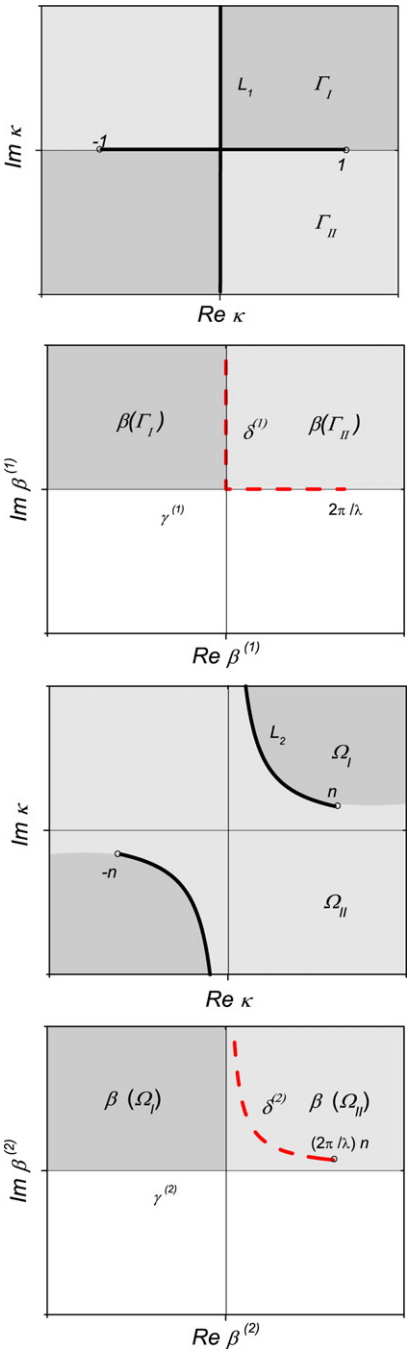

Fig. 2. (a) Cut line L_1 divides regions Γ_I (dark grey) and Γ_{II} (light grey). (b) Branch of function $\beta^{(1)}(\kappa)$: $\mathrm{Im}\,\beta^{(1)} \geq 0$. Curve $\delta^{(1)}$ (dotted lines) represents $\beta^{(1)}$ values for real values of κ. (c) Cut line L_2 divides regions Ω_I (dark grey) and Ω_{II} (light grey). (d) Branch of function $\beta_m^{(2)}(\kappa)$: $\mathrm{Im}\,\beta^{(2)} \geq 0$. Curve $\delta^{(2)}$ (dotted lines) represents $\beta^{(2)}$ values for real values of κ.

Please cite this article in press as: M. Cuevas, R.A. Depine, The homogeneous problem for a corrugated metamaterial of arbitrary permittivity and permeability: Choosing the proper Riemann surface, Optik - Int. J. Light Electron Opt. (2010), doi:10.1016/j.ijleo.2009.12.010

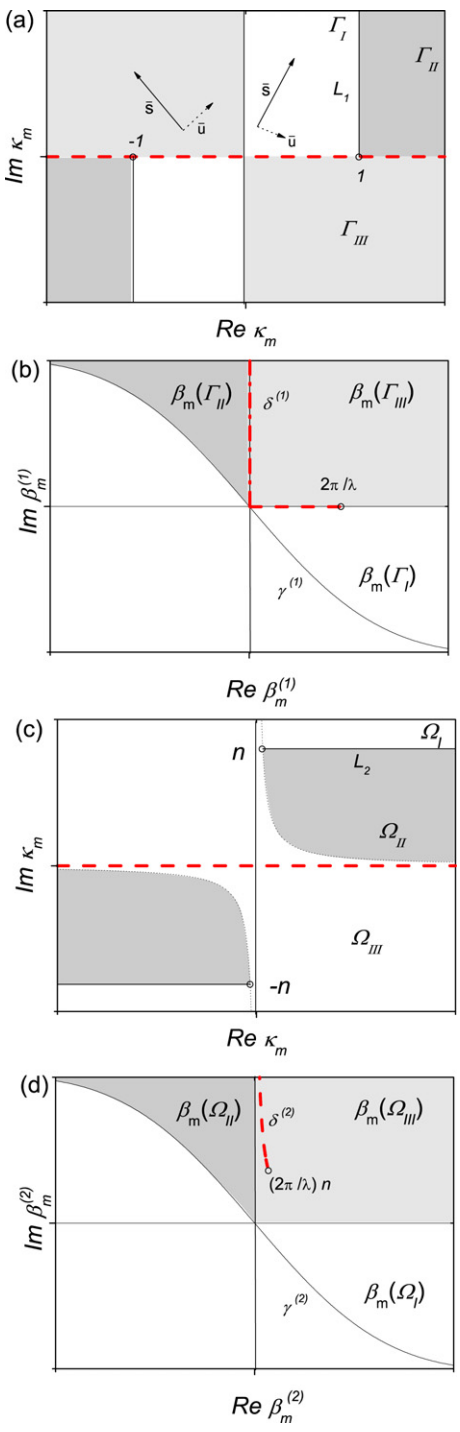

Fig. 3. (a) Cut line L_1, drawn from the branch points $\kappa_m = \pm 1$ according to condition (13). The cut line divides regions Γ_I (dark grey) and Γ_{II} (light grey). Vectors $\bar{s}$ and $\bar{u}$ represent the propagation and decay directions respectively, corresponding to radiative spatial harmonics. (b) $\gamma^{(1)} = \beta_m^{(1)}(L_1)$. The branch of $\beta_m^{(1)}(\kappa)$ is in the region located above curve $\gamma^{(1)}$. Curve $\delta^{(1)}$ (dotted lines) represents $\beta_m^{(1)}$ values for real values of κ. (c) Cut line L_2 divides regions Ω_I (dark grey) and Ω_{II} (light grey). (d) $\gamma^{(2)} = \beta_m^{(2)}(L_2)$. Curve $\delta^{(2)}$ (dotted lines) represents $\beta_m^{(2)}$ values for real values of κ.

surface waves (surface plasmons) described in Eq. (8) can actually propagate with $\kappa(h/d)$ very similar to the propagation constant $\kappa(0)$ corresponding to the plane surface. It is always possible to choose a value of λ/d (for example, by adequately choosing the period of the grating) so that the plasmon has two radiative orders, both of them with outgoing power fluxes in the direction $+y$, as outlined in Fig. 1b. If $\mathrm{Re}\,\kappa > 0$, the main harmonic ($m = 0$) propagates in the direction $+x$, and therefore, $\mathrm{Im}\,\kappa > 0$. In this situation, the power flux associated with the spatial harmonic $m = -1$ has a component in the direction $+x$ ($0 < \kappa_{-1} < 1$) while the power flux associated with the spatial harmonic $m = -2$ has a component in the direction $-x$ ($-1 < \kappa_{-2} < 0$). Although the criterion (12) for choosing cuts correctly predicts the radiation direction associated with the spatial harmonic $m = -2$, this is not the case for the spatial harmonic $m = -1$. This is due to the fact that with this criterion κ_{-1} falls in region Γ_I of Fig. 2a, and then $\beta_{-1}^{(1)}$ falls in region $\beta(\Gamma_I)$ of Fig. 2b. In this region, $\mathrm{Re}\,\beta_{-1}^{(1)} < 0$ (the correct direction of the power flux is not reproduced) and $\mathrm{Im}\,\beta_{-1}^{(1)} > 0$ (the field associated with the harmonic $m = -1$ becomes confined to the surface), and so we must conclude that criterion (12) for choosing the cuts of $\beta_m^{(1)}(\kappa)$ is not physically adequate to deal with the homogeneous problem of corrugated surfaces.

The above example evidences that the adequate cuts to describe physical situations as the one outlined in Fig. 1b must handle spatial harmonics with $|\mathrm{Re}\,\kappa_m| > 1$ differently from those with $|\mathrm{Re}\,\kappa_m| < 1$. This is why the cuts must be similar to the one proposed in [20,2] for the case of conventional media and used by [24] to determine the characteristics of surface waves, both radiative and non-radiative, in a metallic plane slab. Since the cut lines depend on the characteristics of the refractive index of medium 2, we analyze two situations: (A) when medium 2 is reactive (refractive index with a significant imaginary part, waves do not penetrate the medium) and (B) when medium 2 is transparent, with a negative refractive index (negative real part, small imaginary part, waves penetrate the medium).

2.1. When medium 2 is reactive

When medium 2 is reactive, $\mathrm{Re}\,\varepsilon_2\,\mathrm{Re}\,\mu_2 < 0$, the surface wave can only radiate into medium 1. This situation includes p polarized plasmons that can propagate along conventional metallic media ($\mathrm{Re}\,\varepsilon_2 < 0, Re\,\mu_2 > 0$) and s polarized surface waves that can propagate along metamaterials with $\mathrm{Re}\,\varepsilon_2 > 0$ and $Re\,\mu_2 < 0$. In the previous example, cut (12) assigns $\mathrm{Re}\,\beta_{-1}^{(1)} < 0$ when $\mathrm{Re}\,\kappa_{-1} < 1$, leading to an inadequate result, i.e. the spatial harmonic $m = -1$ cannot radiate into medium 1. To avoid this problem, the cut line must be chosen so that $\beta_m^{(1)}$ changes its sign when κ_m crosses the line $\mathrm{Re}\,\kappa_m = 1$. One of the simplest cuts to correctly describe the physical situation outlined in Fig. 1b is to define the vertical lines drawn from the branch points $\kappa_m = \pm 1$ as cut lines, according to the condition:

$$\mathrm{Re}\,\kappa_m = \pm 1, \quad \mathrm{Re}\,\kappa_m \mathrm{Im}\,\kappa_m \geq 0. \tag{13}$$

Fig. 3 shows cut lines (13) represented by the symbol L_1 and Fig. 3b shows the image of this line $\gamma^{(1)} = \beta_m^{(1)}(L_1)$ in the complex plane $\beta_m^{(1)}$. The analytic continuation of function $\beta_m^{(1)}(\kappa)$ requires that its branch include the image of the real axis of plane κ_m, represented by the symbol $\delta^{(1)}$ in Fig. 3b. To do this, the branch of function $\beta_m^{(1)}(\kappa)$ must match the region located above curve $\gamma^{(1)}$. In the limit $\mathrm{Im}\,\kappa \ll 1$, as is the case for a small intrinsic loss of the medium, curve $\gamma^{(1)}$ in Fig. 3b can be approximated by a straight line $\mathrm{Re}\,\beta_m^{(1)} + \mathrm{Im}\,\beta_m^{(1)} = 0$, which is a procedure used in the cuts proposed in Refs. [20,2] for the study of plasmons. In this approximation, the branch of the function is

$$\mathrm{Re}\,\beta_m^{(1)} + \mathrm{Im}\,\beta_m^{(1)} \geq 0, \tag{14}$$

while the cut line (pre-image of line $\mathrm{Re}\,\beta_m^{(1)} + \mathrm{Im}\,\beta_m^{(1)} = 0$) can be approximated by the expression:

$$\kappa_m^2 - 1 = i\,a, \quad \text{where } a \text{ is real and positive.} \tag{15}$$

Please cite this article in press as: M. Cuevas, R.A. Depine, The homogeneous problem for a corrugated metamaterial of arbitrary permittivity and permeability: Choosing the proper Riemann surface, Optik - Int. J. Light Electron Opt. (2010), doi:10.1016/j.ijleo.2009.12.010

Similarly, the cut line for the function $\beta_m^{(2)}$ can be chosen:

$$\kappa_m^2 - n = i\,a, \quad \text{where } a \text{ is real and positive,} \tag{16}$$

and, consequently, the branch of the function $\beta^{(2)}$ becomes

$$\mathrm{Re}\,\beta_m^{(2)} + \mathrm{Im}\,\beta_m^{(2)} \geq 0. \tag{17}$$

Since the relative refractive index is almost imaginary, κ does not cross these cut lines because they are too far away from the real axis. Therefore, condition (17) can be replaced with the branch of the function corresponding to the plane case:

$$\mathrm{Im}\,\beta_m^{(2)} \geq 0. \tag{18}$$

The infinite set of planes κ_m whose image through functions $\beta_m^{(j)}$ is determined by conditions (14) and (17) or (14) and (18) constitutes the Riemann physical sheet of the problem. In Fig. 3a, we have represented the propagation direction $\bar{s}$ and the decay direction $\bar{u}$ for spatial harmonics with κ_m in regions Γ_I and Γ_{III}, with $|\mathrm{Re}\,\kappa_m| < 1$ and $\mathrm{Im}\,\kappa > 0$, in accordance with the branch of the parameter $\beta_m^{(1)}$ represented in Fig. 3b. It should be noted that this branch provides the correct radiation direction in medium 1, outlined in Fig. 1b. Fig. 3c shows that κ_m belongs to regions Ω_{II} or Ω_{III}. Consequently, $\mathrm{Im}\,\beta_m^{(2)} \geq 0$, and so the spatial harmonics become confined to the surface.

2.2. When medium 2 has a negative refractive index

In this case, surface waves can also radiate into medium 2, a novel characteristic that makes them different from surface waves in conventional materials. In the dispersion problem (real κ_m), the parameters $\beta_m^{(2)}$ must be chosen in accordance with conditions [22] to satisfy the radiation condition at infinity

$$\mathrm{Im}\beta_m^{(2)} \geq 0, \tag{19}$$

and thus function $\beta_m^{(2)}$ moves along the curve $\delta^{(2)}$ represented by a dotted line in Fig. 4d. With this condition, and in the ideal lossless case, the spatial harmonics in medium 2 are radiative, with the power flux in the $-y$ direction when $n < \kappa_m < -n$ and $\beta_m^{(2)}$ is real and negative, or non-radiative, with fields confined to the surface when $|\kappa_m| > -n$ and $\beta_m^{(2)}$ is a positive imaginary number. To generalize condition (19) to complex values of κ_m, the cut line can be drawn from the branch points $\kappa = \pm n$, just as we did for condition (13)

$$\mathrm{Re}\,\kappa_m = \pm \mathrm{Re}\,n, \quad \mathrm{Re}\,\kappa_m\,\mathrm{Im}\,\kappa_m \leq \mathrm{Re}\,n\,\mathrm{Im}\,n. \tag{20}$$

In this cut line definition, we have considered the most general case, in which the medium has a small loss. Fig. 4c and d show cut line L_2 and its image in the $\beta_m^{(2)}$ plane, represented by the symbol $\gamma^{(2)}$. The analytic continuation of function $\beta_m^{(2)}(\kappa_m)$ requires that its branch include condition (19). Therefore, the branch of the function must be chosen as the region of the plane above curve $\gamma^{(2)}$. If κ_m is almost a real number, curve $\gamma^{(2)}$ can be approximated by the straight line $-\mathrm{Re}\,\beta_m^{(2)} + \mathrm{Im}\,\beta_m^{(2)} = 0$. In this approximation, the branch of the function can be written as

$$-\mathrm{Re}\,\beta_m^{(2)} + \mathrm{Im}\,\beta_m^{(2)} \geq 0, \tag{21}$$

and the equation corresponding to the cut line becomes

$$\kappa_m^2 - n^2 = -i\,a, \text{ where } a \text{ is real and positive.} \tag{22}$$

To show the Riemann physical sheet corresponding to the dispersion problem of the corrugated interface when medium 1 is an ideal dielectric, we have incorporated Fig. 4a and b showing cut lines L_1 from the branch points $\kappa_m = \pm 1$ and the branches of the function $\beta_m^{(1)}$. In the ideal limit, the cut represented by Eq. (22) coincides with

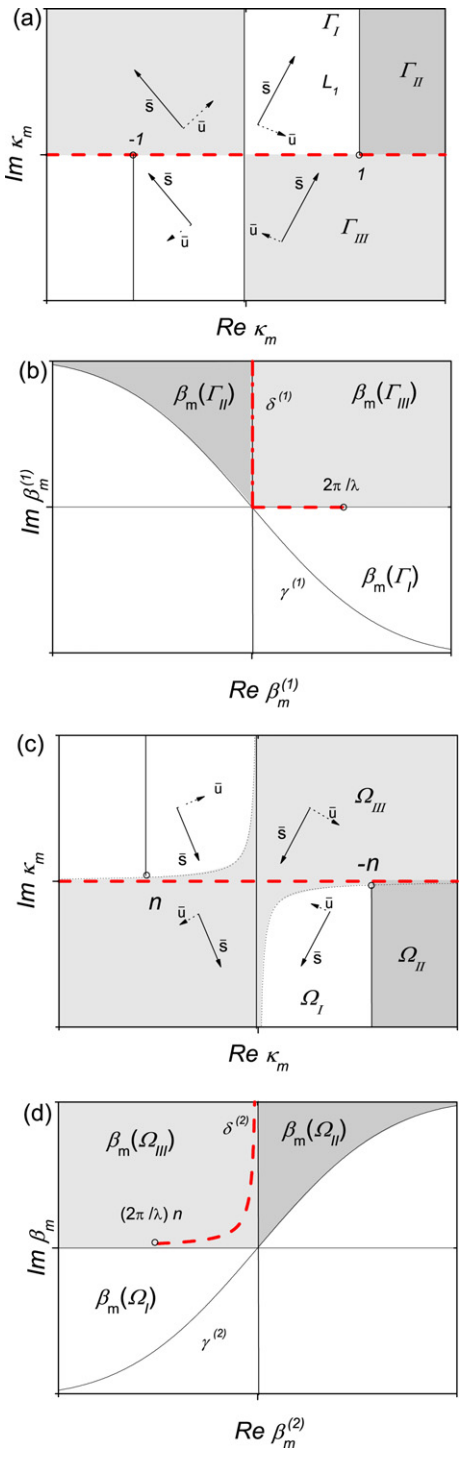

Fig. 4. (a) Cut line L_1, drawn from the branch points $\kappa_m = \pm 1$ according to condition Eq. (20). The cut line divides regions Γ_I (dark grey) and Γ_{II} (light grey). Vectors $\bar{s}$ and $\bar{u}$ represent the propagation and decay directions respectively, corresponding to radiative spatial harmonics. (b) $\gamma^{(1)} = \beta_m^{(1)}(L_1)$. The branch of $\beta_m^{(1)}(\kappa)$ is in the region located above curve $\gamma^{(1)}$. Curve $\delta^{(1)}$ (dotted lines) represents $\beta_m^{(1)}$ values for real values of κ. (c) Cut line L_2 drawn from the branch points $\kappa_m = \pm n$ according to condition Eq. (20). The cut line divides regions Γ_I (dark grey) and Γ_{II} (light grey). Vectors $\bar{s}$ and $\bar{u}$ represent the propagation and decay directions respectively, corresponding to radiative spatial harmonics. (d) $\gamma^{(2)} = \beta_m^{(2)}(L_2)$. Curve $\delta^{(2)}$ (dotted lines) represents $\beta_m^{(2)}$ values for real values of κ.

Please cite this article in press as: M. Cuevas, R.A. Depine, The homogeneous problem for a corrugated metamaterial of arbitrary permittivity and permeability: Choosing the proper Riemann surface, Optik - Int. J. Light Electron Opt. (2010), doi:10.1016/j.ijleo.2009.12.010

that proposed in [23]. In this limit, the surface wave can radiate energy into medium 2 (in the $-y$ direction) through those spatial harmonics satisfying $n < \mathrm{Re}\,\kappa_m < -n$.

To see the characteristics of the power flux radiated by the surface wave, let us assume that the spatial harmonic m belongs to the radiative area contained in region Ω_{III} (Fig. 4c). In this case, conditions $0 < \mathrm{Re}\,\kappa_m < -n$, $\mathrm{Im}\kappa > 0$, or $n < \mathrm{Re}\,\kappa_m < 0$, $\mathrm{Im}\kappa < 0$ are verified, and so $\beta_m^{(2)}$ falls in region $\beta_m^{(2)}(\Omega_{III})$ of Fig. 4d. In this region, $\mathrm{Re}\,\beta_m^{(2)} < 0$, therefore the power flux associated with this spatial harmonic is in the $-y$ direction ($\varepsilon_2 < 0$, $\mu_2 < 0$). Besides, each spatial harmonic m verifies the dispersion relation

$$\alpha_m^2 + \beta_m^2 = \left(\frac{\omega}{c}\right)^2 \varepsilon_2 \mu_2. \tag{23}$$

Since the imaginary part of this equation is zero, $\mathrm{Re}\,\alpha_m\,\mathrm{Im}\,\alpha_m + \mathrm{Re}\,\beta_m\,\mathrm{Im}\,\beta_m = 0$ and therefore the direction of the power flux radiated into medium 2 is perpendicular to the attenuation direction. Fig. 4c shows the radiation and attenuation direction with vectors $\bar{s}$ and $\bar{u}$ respectively. To represent vector $\bar{u}$, we have taken into account the sign of $\mathrm{Im}\,\kappa_m$ and the sign of $\mathrm{Im}\,\beta_m^{(2)}$. A similar analysis enables us to infer the radiation and attenuation direction represented in Fig. 4c, for κ_m belonging to region Ω_I. In the ideal limit, the power flux radiated into medium 2 has the same characteristics as the flux radiated into medium 1 when the surface wave propagates along a metallic corrugation. The scheme of vectors $\bar{s}$ and $\bar{u}$ shown in Fig. 4a and c illustrates how the surface wave loses energy through radiation – into medium 1 and medium 2 – when it propagates along the corrugated surface. The spatially transient wave characteristic of the radiation field is also characteristic of the field radiated by surface plasmons in plane slabs [24,25].

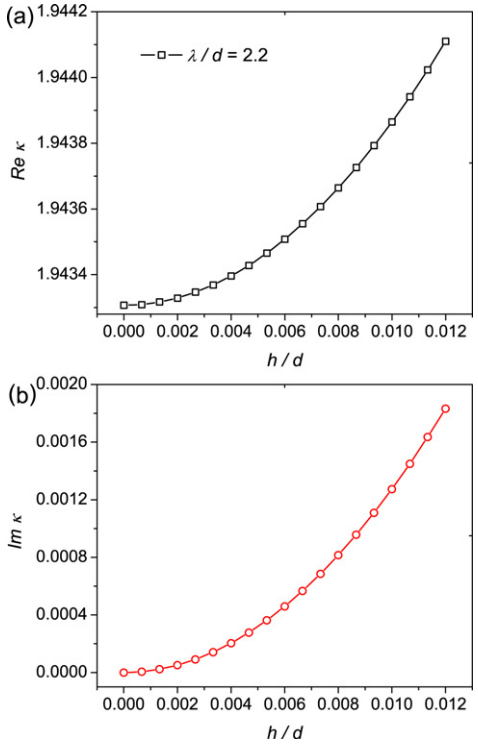

Fig. 5. Real (a) and imaginary (b) parts of the propagation constant κ as a function of h/d. Constitutive parameters corresponding to regime A ($\varepsilon = -0.176$, $\mu = -1.135$) and $\lambda/d = 2.2$.

3. Dispersion relation

To find the surface wave characteristics of the periodically corrugated surface, we have developed a perturbative method valid for weak corrugation ($h/\lambda \ll 1$) and similar to the one presented in [21] for magnetic media with positive refractive index. Taking into account that for $h = 0$ the surface wave is described by the spatial harmonic with $m = 0$, the amplitude corresponding to this harmonic results O(1) in the weak corrugation limit, while the amplitudes for harmonics with $m \neq 0$ are at least O(h/λ). By retaining the first-order terms in the series (8) the dispersion relation for the spatial harmonic $m = 0$ is written as:

$$M_{00} = \beta_0^{(2)} + \sigma\beta_0^{(1)}$$
$$= -\sum_{m\neq 0} \frac{M_{0m}M_{m0}}{M_{mm}} (\beta_m^{(1)} - \beta_0^{(2)})(\beta_0^{(1)} - \beta_m^{(2)}) |\xi^{(1)}(m)|^2, \tag{24}$$

where $\sigma = \varepsilon$ for p polarization and $\sigma = \mu$ for s polarization. The matrix

$$M_{mn} = \beta_n^{(2)} + \sigma\beta_m^{(1)} + \frac{(\alpha_m + \sigma\alpha_n)(\alpha_m - \alpha_n)}{\beta_m^{(1)} - \beta_n^{(2)}}, \tag{25}$$

and $\xi^{(1)}(m)$ is m th Fourier coefficient of function $f(x)$. To calculate $\kappa(h/\lambda)$ with Eq. (24) it is essential to use the analytic continuation developed in the previous section. We apply the formalism in the regions of constitutive parameters $\varepsilon - \mu$ where the flat surface supports surface waves and we observe how the propagation characteristics are modified when the surface is sinusoidally perturbed. If the surface is reactive (relative refractive index mostly imaginary), the solution to Eq. (24) must be found in the proper Riemann sheet defined in Fig. 3, whereas if the medium is transparent (relative refractive index mostly real), the solution to Eq. (24) must be found in the proper Riemann sheet defined in Fig. 4. Here we restrict ourselves to obtaining the proper modes for regimes in which the medium is transparent. These regimes are described in Refs. [9,10] and correspond to constitutive parameters characterized by the following conditions:

- Regime A: $\varepsilon > -1$, $\mu < -1$, $\varepsilon\,\mu < 1$, s polarization
- Regime B: $\varepsilon > -1$, $\mu < -1$, $\varepsilon\,\mu > 1$, p polarization
- Regime C: $\varepsilon < -1$, $\mu > -1$, $\varepsilon\,\mu > 1$, s polarization
- Regime D: $\varepsilon < -1$, $\mu > -1$, $\varepsilon\,\mu < 1$, p polarization

Given that regimes C and D are obtained from regimes A and B by interchanging the constitutive parameters $\varepsilon \leftrightarrow \mu$ as well as the polarization $p \leftrightarrow s$, we will show the effect of corrugation on the surface wave characteristics in regions A and B.

3.1. Regime A

In this section, we implement the formalism developed in the previous sections. Specifically, we determine the Riemann physical sheet for transparent media. This sheet allows us to find the propagation constant κ which solves Eq. (24) and has a physical sense. The graphic representation of each radiative spatial harmonic κ_m, Fig. 4a and c, offers valuable insight into the novel propagation properties of surface waves in this regime. To illustrate these properties, we consider a sinusoidal surface with relative constitutive parameters $\varepsilon = -0.176$, $\mu = -1.135$ ($n = -0.447$). We choose the relation $\lambda/d = 2.2$. For the case $h = 0$ the surface wave has s polarization and the net power flux is in the same direction as the propagation parameter $\kappa(0)$. For this reason, the surface waves in this regime are also called *forward surface polaritons* [9,10]. Fig. 5a and b shows respectively the real and imaginary parts of κ as a function of h. Starting with the value corresponding to the plane surface $\kappa(0) = 1.9433$, the values of $\mathrm{Re}\,\kappa(h/d)$ and $\mathrm{Im}\,\kappa(h/d)$ increase with h/d and consequently, the power flux radiated also increases. Since the media have no intrinsic losses, the non zero value of $\mathrm{Im}\,\kappa(h/d)$

Please cite this article in press as: M. Cuevas, R.A. Depine, The homogeneous problem for a corrugated metamaterial of arbitrary permittivity and permeability: Choosing the proper Riemann surface, Optik - Int. J. Light Electron Opt. (2010), doi:10.1016/j.ijleo.2009.12.010

is explained by the fact that the surface wave radiates energy as it propagates along the surface. Fig. 5b shows that this value increases with h/d, and consequently the radiated power flux also increases.

Fig. 6a shows the flux lines and the absolute value of the Poynting vector, illustrated here with a color pallet for $h/d = 0.012$. Near the surface, the characteristics of the surface wave are similar to the case $h = 0$: the flux lines are almost parallel to the surface, in the $+x$ direction in medium 1 and in the $-x$ direction in medium 2. This is due to the fact that the amplitudes R_m with $m \neq 0$ in Eq. (8) are $O(h/\lambda)$, whereas R_0 is $O(1)$. Therefore, the field near the surface is quite similar to the field corresponding to the plane surface, except that in the latter case the propagation constant is real, and so the surface wave does not lose energy when it propagates.

The perturbation induces a radiative spatial harmonic with $m = -1$ ($-1 < \mathrm{Re}\,\kappa_{-1} < 0$) (Eq. (8)) which is manifested in the flux shown in Fig. 6a by the radiation lines in the outgoing direction. This is due to the fact that κ_{-1} falls in region Γ_{III} of Fig. 4a, with $\mathrm{Im}\,\kappa > 0$, and then $\beta_{-1}^{(1)}$ falls in region $\beta_{-1}^{(1)}(\Gamma_{III})$ of Fig. 4b. In this region, $\mathrm{Re}\,\beta^{(1)} > 0$ (the radiated power flux is in the $+y$ direction). Furthermore, κ_{-1} falls in region Ω_I of Fig. 4c with $\mathrm{Im}\,\kappa > 0$, and then $\beta_{-1}^{(2)}$ falls in region $\beta_{-1}^{(2)}(\Omega_I)$ of Fig. 4d. Therefore $\mathrm{Re}\,\beta_{-1}^{(2)} < 0$ (the radiated power flux is in the $-y$ direction in medium 2). Since this flux results from the energy loss of the surface wave, it does not present the same characteristics as the flux of a plane wave, as its intensity decreases in the $+x$ direction ($\mathrm{Im}\,\kappa > 0$). To understand the spatial characteristics of the radiation flux, we should observe Fig. 4, which shows the radiation direction $\bar{s}$ and the attenuation direction $\bar{u}$ for κ_{-1} belonging to the radiative regions Γ_{III} and Ω_I with $\mathrm{Im}\,\kappa_{-1} > 0$. Since these directions are perpendicular to one another, the absolute value of the Poynting vector (intensity) remains constant along each radiation line shown in Fig. 6a. Because the x component of $\bar{u}$ is positive, this intensity decreases from one line to another in the +x direction. These two assertions have been numerically verified. Note that the flux lines radiated into medium 1 and medium 2 do not emerge on the same side of the y axis.

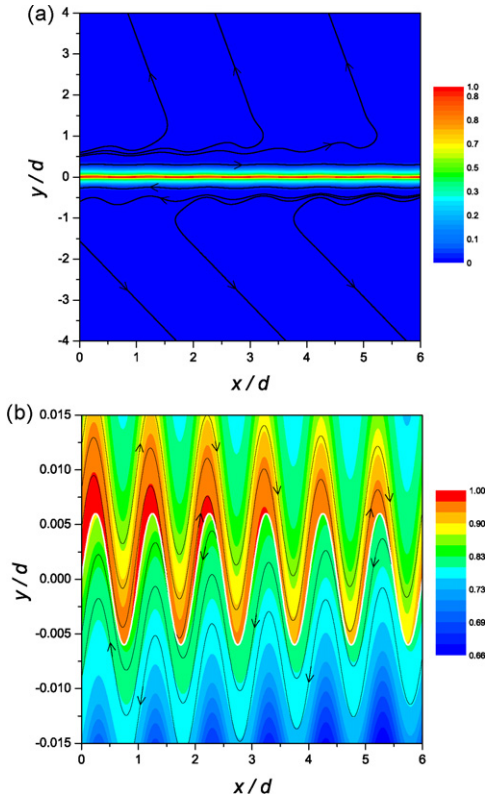

Fig. 6. (a) Flux lines and modulus of the Poynting vector (illustrated with a color pallet) for $h/d = 0.012$. (b) Flux lines and modulus of the Poynting vector near the surface. Constitutive parameters corresponding to regime A ($\varepsilon = -0.176$, $\mu = -1.135$) and $\lambda/d = 2.2$.

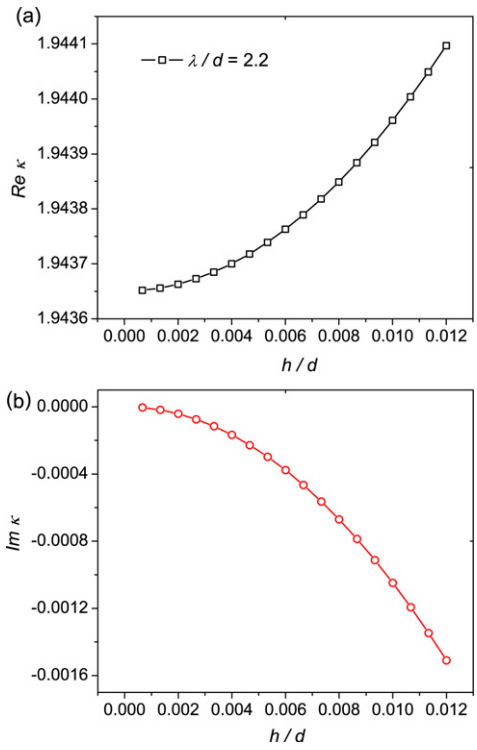

Fig. 7. Real (a) and imaginary (b) parts of the propagation constant κ as a function of h/d for constitutive parameters corresponding to regime B ($\varepsilon = -0.8$, $\mu = -2.5$) and $\lambda/d = 2.2$.

Fig. 6b shows the flux lines and the absolute value of the Poynting vector near the surface. As in the case of the plane surface, the energy is mostly concentrated on medium 1, in agreement with the forward nature of the surface wave in this regime. However, contrary to the case of $h = 0$, we observe that the flux lines penetrate the surface. This is due to the fact that the surface wave loses energy in the $+x$ direction and, as a result, a net flux in the $-y$ direction appears. The colored map in Fig. 6b clearly shows that the intensity decreases in the $+x$ direction. This decrease (and consequently the flux normal to the surface) also appears in the $h = 0$ case when a lossy medium is considered.

3.2. Regime B

If $h = 0$, the direction of the net power flux of surface waves is antiparallel to the propagation direction. This is why the proper modes are also known as *backward surface polaritons* [9,10]. To observe substantial changes in these proper modes when the surface is slightly corrugated, we choose the constitutive parameters $\varepsilon = -0.8$, $\mu = -2.5$ ($n = -1.414$) and the same λ/d relation as the previous case. Fig. 7a shows that the real part of the propagation constant increases with the corrugation amplitude. Starting from the value $\kappa(0) = 1.9436$, we observe that the value of $\mathrm{Re}\,\kappa(h/d)$ increases as in the previous case. Since the surface wave radiates energy as it propagates along the surface, $|\mathrm{Im}\,\kappa(h/d)|$ also increases, except that now $\mathrm{Im}\,\kappa(h/d)$ is negative. The negative value of the product $\mathrm{Re}\,\kappa\,\mathrm{Im}\,\kappa$ is a characteristic of the backward regime, also present in the case of $h = 0$ when lossy media are considered [11].

Fig. 8a shows the flux lines and the absolute value of the Poynting vector for $h/d = 0.012$. As in the previous case, the flux lines

Please cite this article in press as: M. Cuevas, R.A. Depine, The homogeneous problem for a corrugated metamaterial of arbitrary permittivity and permeability: Choosing the proper Riemann surface, Optik - Int. J. Light Electron Opt. (2010), doi:10.1016/j.ijleo.2009.12.010

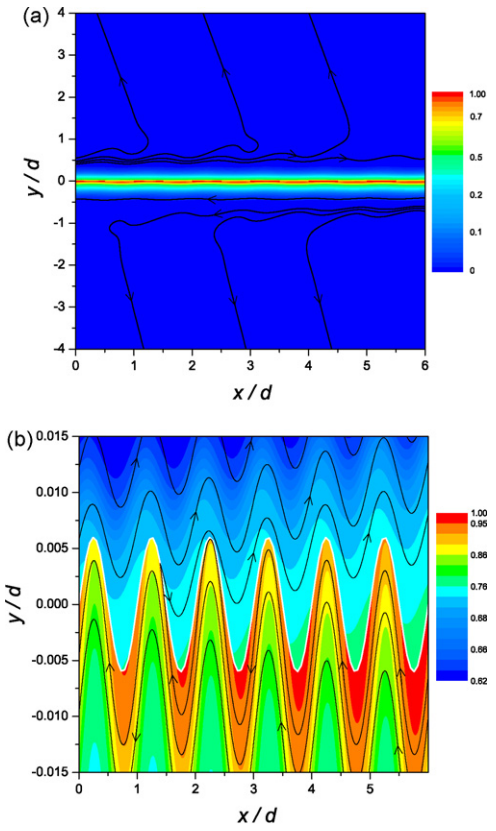

Fig. 8. (a) Flux lines and modulus of the Poynting vector (illustrated with a color pallet) for $h/d = 0.012$. (b) Flux lines and modulus of the Poynting vector near the surface. Constitutive parameters corresponding to regime B ($\varepsilon = -0.8$, $\mu = -2.5$) and $\lambda/d = 2.2$.

near the surface are almost parallel to the surface: in the $+x$ direction in medium 1 and in the $-x$ direction in medium 2. The perturbation induces a radiative spatial harmonic with $m = -1$ which is manifested in the flux lines shown in Fig. 8a. Since the value of the real part of the propagation constant is almost the same as in the previous case and the value of λ/d is the same for both cases, the flux lines are radiated into the dielectric medium with almost the same inclination with the y axis. However, since κ_{-1} falls in the radiative region Γ_I with $\mathrm{Im}\,\kappa_{-1} < 0$ of Fig. 4a, the attenuation direction $\bar{u}$ (which is perpendicular to the radiation direction $\bar{s}$) has a $-x$ component. Furthermore, since κ_{-1} also belongs to region Ω_{III} with $\mathrm{Im}\,\kappa_{-1} < 0$, the flux is radiated into medium 2 in the outgoing direction $\bar{s}$ (Fig. 4c).

In Fig. 4c, we can also observe that the attenuation direction $\bar{u}$ has an $-x$ component. We have numerically verified that the intensity remains constant for $|y/d| > 3$ on each radiation line shown in Fig. 8a and that this intensity decreases from one line to another in the $-x$ direction. Therefore, the radiated intensity decreases in both medium 1 and medium 2 in the $-x$ direction, which is opposite to the propagation direction $+x$.

Fig. 8b shows the flux lines and the absolute value of the Poynting vector near the surface. In this case, the highest intensity is concentrated on the metamaterial side, as opposed to the dielectric side, as in the previous regime. Besides, we can observe flux lines passing through the surface, except that now the flux is in the $+y$ direction. This is so because $\mathrm{Im}\,\kappa < 0$. The same situation is obtained for the case $h = 0$, when the negative imaginary part of the propagation constant results from the intrinsic losses of the metamaterial medium.

4. Conclusion

We have extended to the complex plane the solution to the boundary-value problem for a metamaterial grating. We observed that the cuts chosen to analyze the homogeneous problem associated with a plane surface are not adequate to solve the problem of a weakly corrugated surface. We have generalized the cuts proposed for metallic corrugations to the case of metamaterial media and we have built the Riemann physical sheet. The changes introduced by the presence of corrugation in the propagation characteristics of surface waves have been discussed in terms of the different regions of the physical sheet. In particular, we have seen that the presence of a corrugation can induce radiative spatial harmonics, through which the surface wave loses energy. This energy loss may be attenuated in the propagation direction (forward surface waves) or in the opposite direction (backward surface waves). We have shown that the radiation direction on both sides of the corrugation do not emerge on the same side of the normal to the mean plane of the surface, in agreement to the fact that the surface is negatively refracting.

For forward surface waves, a flux penetrates the metamaterial medium from the dielectric medium. This flux is a consequence of the fact that the surface wave loses energy as it propagates. On the other hand, for backward surface waves, this flux penetrates the dielectric medium from the metamaterial medium because the surface wave loses energy in the direction opposite to the propagation direction. Furthermore, we have shown that the forward surface waves concentrate most of their energy on the dielectric medium, as is the case of surface plasmons, whereas the backward surface waves concentrate most of their energy on the metamaterial medium.

References

[1] U. Fano, The theory of anomalous diffraction gratings and of quasi-stationary waves on metallic surfaces (Sommerfeld's waves), J. Opt. Soc. Am. 31 (1941) 213–222.
[2] D. Maystre, in: A.D. Boardman (Ed.), Electromagnetic Surface Modes, Wiley, New York, 1982.
[3] H. Raether, Surface Plasmons on Smooth and Rough Surfaces and on Gratings, Springer Verlag, Berlin, 1986.
[4] R. Ruppin, Surface polaritons of a left-handed medium, Phys. Lett. A 277 (2000) 61–64.
[5] J. Pendry, Focus issue: negative refraction and metamaterials, Opt. Exp. 11 (2003) 639.
[6] T. Itoh, A.A. Oliner, Special issue on metamaterial structures, phenomena and applications, IEEE Transactions on Microwave Theory and Techniques 52 (2005) 1418.
[7] V.M. Shalaev, A. Boardman, Focus issue on metamaterials, J. Opt. Soc. Am. B 23 (2006) 386–387.
[8] N. Engheta, R.W. Ziolkowski (Eds.), Metamaterials: Physics and Engineering Explorations, Wiley-IEEE Press, 2006.
[9] S.A. Darmanyan, M. Nevière, A.A. Zakhidov, Surface modes at the interface of conventional and left-handed media, Opt. Commun. (2003) 225–233.
[10] I. Shadrivov, A. Sukhorukov, I. Kivshar, A. Zharov, A. Boardman, P. Egan, Nonlinear surfaces waves in left-handed materials, Phys. Rev. E 69 (2004) 016617.
[11] A. Ishimaru, J.R. Thomas, S. Jaruwatanadilok, Electromagnetic waves over half-space metamaterials of arbitrary permittivity and permeability, IEEE Trans. Antennas Propag 53 (2005) 915–921.
[12] F. Yang, J.R. Sambles, G.W. Bradberry, Long-range coupled surface exciton polaritons, Phys. Rev. Lett. 64 (1990) 559–562.
[13] M. Sarrazin, J.P. Vigneron, Light transmission assisted by Brewster–Zennek modes in chromium films carrying a subwavelength hole array, Phys. Rev. B 71 (2005) 075404.
[14] F. Miyamaru, M. Tanaka, M. Hangyo, Resonant electromagnetic wave transmission through strontium titanate hole arrays with complex surface waves, Phys. Rev. B 74 (2006) 115117.
[15] E. Popov, S. Enoch, M. Nevière, Plasmon surface waves and complex-type surface waves: comparative analysis of single interfaces, lamellar gratings, and two-dimensional hole arrays, Appl. Opt. 46 (2007) 154–160.
[16] M. Cuevas, R.A. Depine, Excitation of surface plasmon polaritons along the sinusoidal boundary of a metamaterial, Phys. Rev. B 78 (2008) 125412.
[17] A. Sommerfeld, Propagation of waves in wireless telegraphy, Ann. Phys. 28 (1909) 665–736.

Please cite this article in press as: M. Cuevas, R.A. Depine, The homogeneous problem for a corrugated metamaterial of arbitrary permittivity and permeability: Choosing the proper Riemann surface, Optik - Int. J. Light Electron Opt. (2010), doi:10.1016/j.ijleo.2009.12.010

[18] J. Zenneck, Propagation of plane EM waves along a plane conducting surface, Ann. Phys. 23 (1907) 846–866.
[19] R.E. Collin, Hertzian dipole radiating over a lossy earth or sea: some early and late 20th-century controversies, IEEE Antennas Propag Mag 46 (2004) 64–79.
[20] M. Nevière, The homogeneus problem, in: E. Petit (Ed.), Electromagnetic Theory of Gratings, Springer Verlag, New York, 1980.
[21] M. Lester, R.A. Depine, Scattering of electromagnetic waves at the corrugated interface between index-matched media, Opt. Commun. (1996) 132–135.
[22] R.A. Depine, A. Lakhtakia, Diffraction gratings of isotropic negative-phase velocity materials, Optik 116 (2005) 31–43.
[23] P. Melezhik, A. Poyedinchuk, N. Yashina, G. Granet, J. Opt. A: Pure Appl. Opt. 9 (2007) 403–409.
[24] J.J. Burke, G.I. Stegeman, T. Tamir, Surface-polariton-like waves guided by thin, lossy metal films, Phys. Rev. B 33 (1986) 5186–5201.
[25] D. Marcuse, Theory of Dielectric Optical Waveguides, Academic Press, Inc., 1974.

Please cite this article in press as: M. Cuevas, R.A. Depine, The homogeneous problem for a corrugated metamaterial of arbitrary permittivity and permeability: Choosing the proper Riemann surface, Optik - Int. J. Light Electron Opt. (2010), doi:10.1016/j.ijleo.2009.12.010